Estrogen induces two distinct cholesterol crystallization pathways by activating ERα and GPR30 in female mice

Ornella de Bari,* Tony Y. Wang,*,[†] Min Liu,[§] Piero Portincasa,** and David Q-H. Wang[1],*

Department of Internal Medicine,* Division of Gastroenterology and Hepatology, Saint Louis University School of Medicine, St. Louis, MO 63104; Department of Biomedical Engineering,[†] Washington University, St. Louis, MO 63130; Department of Pathology and Laboratory Medicine,[§] University of Cincinnati College of Medicine, Cincinnati, OH 45237; and Clinica Medica "A. Murri," Department of Biomedical Sciences and Human Oncology,** University of Bari Medical School, Bari, Italy

Abstract To distinguish the lithogenic effect of the classical estrogen receptor α (ERα) from that of the G protein-coupled receptor 30 (GPR30), a new estrogen receptor, on estrogen-induced gallstones, we investigated the entire spectrum of cholesterol crystallization pathways and sequences during the early stage of gallstone formation in gallbladder bile of ovariectomized female wild-type, GPR30($^{-/-}$), ERα($^{-/-}$), and GPR30($^{-/-}$)/ERα($^{-/-}$) mice treated with 17β-estradiol (E_2) at 6 μg/day and fed a lithogenic diet for 12 days. E_2 disrupted biliary cholesterol and bile salt metabolism through ERα and GPR30, leading to supersaturated bile and predisposing to the precipitation of cholesterol monohydrate crystals. In GPR30($^{-/-}$) mice, arc-like and tubular crystals formed first, followed by classical parallelogram-shaped cholesterol monohydrate crystals. In ERα($^{-/-}$) mice, precipitation of lamellar liquid crystals, typified by birefringent multilamellar vesicles, appeared earlier than cholesterol monohydrate crystals. Both crystallization pathways were accelerated in wild-type mice with the activation of GPR30 and ERα by E_2. However, cholesterol crystallization was drastically retarded in GPR30($^{-/-}$)/ERα($^{-/-}$) mice.▪ We concluded that E_2 activates GPR30 and ERα to produce liquid crystalline versus anhydrous crystalline metastable intermediates evolving to cholesterol monohydrate crystals from supersaturated bile. GPR30 produces a synergistic lithogenic action with ERα to enhance E_2-induced gallstone formation.—de Bari, O., T. Y. Wang, M. Liu, P. Portincasa, and D. Q-H. Wang. **Estrogen induces two distinct cholesterol crystallization pathways by activating ERα and GPR30 in female mice.** *J. Lipid Res.* 2015. **56:** 1691–1700.

Supplementary key words bile flow • bile salt • biliary secretion • *Lith* gene • micelle • vesicle • estrogen receptor subtype α • G protein-coupled receptor 30

The precipitation of classical parallelogram-shaped cholesterol monohydrate crystals from supersaturated gallbladder bile is the first irreversible physical-chemical event during the early stage of cholesterol gallstone formation (1). It is well known that estrogen has a critical role in the pathogenesis of cholesterol cholelithiasis because gallstone prevalence is markedly higher in women than in men at all ages in every population studied (2). Many clinical studies have found that the use of oral contraceptives and conjugated estrogens in premenopausal and postmenopausal women significantly increases the prevalence of gallstones (3–5). Because elevated estrogen levels have a linear and positive relationship with the duration of gestation, the risk of gallstone formation becomes higher in the third trimester of pregnancy (6). Increasing parity is a risk factor for gallstones, especially in younger women. Similar lithogenic effects are also found in men with prostatic cancer during estrogen therapy (7, 8). These epidemiological and clinical studies have clearly demonstrated that high susceptibility to gallstone formation in women compared with men is related to differences in how the liver metabolizes cholesterol in response to estrogen (9).

We have found that the classical estrogen receptor α (ERα), but not ERβ, in the liver plays a critical role in the pathogenesis of 17β-estradiol (E_2)-induced gallstones in female mice (10). Despite these observations, the metabolic abnormalities underlying the lithogenic effect of E_2 on gallstone formation is not fully understood because the targeted deletion of the *Erα* gene cannot completely protect against gallstone formation in ovariectomized (OVX) female mice treated with high doses of E_2 (11). Moreover, the discovery of the G protein-coupled receptor 30 (GPR30), a novel estrogen receptor, has led to a new question of whether it is involved in the lithogenic effect of E_2

Abbreviations: CCK-1R, cholecystokinin-1 receptor; CSI, cholesterol saturation index; E_2, 17β-estradiol; ERα, estrogen receptor subtype α; ERβ, ER subtype β; GPR30, G protein-coupled receptor 30; OVX, ovariectomized.
[1] To whom correspondence should be addressed.
  e-mail: dwang15@slu.edu

on gallstone formation (12). Because E_2 can efficiently bind to and activate both GPR30 and ERα, it is crucial to explore how E_2, through GPR30, ERα, or both, influences the biliary and gallstone phenotypes. The genetic analysis with quantitative trait locus mapping techniques in mice supports the candidacy of *Gpr30* for a new gallstone gene, *Lith18* (13–15). However, little information is available about the underlying lithogenic effect of GPR30 on gallstone formation. Thus, identifying the lithogenic mechanisms of GPR30 is now a focal point of interest.

In the current study, to dissect the lithogenic effects of GPR30 and ERα on the formation of gallstones, we defined the entire spectrum of cholesterol crystallization pathways during the early stage of gallstone formation by investigating the formation of solid plate-like cholesterol monohydrate crystals and subsequent crystal growth in gallbladder bile of OVX female wild-type mice with intact expression of the *Gpr30* and *Erα* genes as well as GPR30$(^{-/-})$, ERα$(^{-/-})$, and GPR30$(^{-/-})$/ERα$(^{-/-})$ mice treated with E_2 at 6 µg/day and fed a lithogenic diet for 12 days. We hypothesized that after GPR30 and ERα are activated by E_2, GPR30 and ERα disrupt biliary cholesterol and bile salt metabolism through different mechanisms, leading to a failure of cholesterol solubilization in bile. As a result, these alterations induce a distinctly abnormal metastable physical-chemical state of gallbladder bile, thereby predisposing to the formation of solid cholesterol monohydrate crystals through different crystallization pathways. These studies would help distinguish the lithogenic effect of GPR30 from that of ERα, at a physical-chemical level, on enhancing cholelithogenesis.

MATERIALS AND METHODS

Animals and diets

The inbred AKR/J mice of both genders purchased from the Jackson Laboratory (Bar Harbor, ME) were bred to generate female mice for the studies. Although AKR/J mice have been found to be a gallstone-resistant strain, they are still susceptible to E_2-induced cholesterol gallstone formation (10). Although AKR/J mice have intact expression of the *Gpr30*, *Erα*, and *Erβ* genes, expression levels of *Erβ* in the liver are almost undetectable under normal physiological conditions. Hepatic expression of *Erβ* is 50-fold lower than that of *Erα* even under the stimulation of E_2. Thus, the AKR/J strain was used as control mice (i.e., wild-type mice). Other experimental animals included female GPR30$(^{-/-})$, ERα$(^{-/-})$, and GPR30$(^{-/-})$/ERα$(^{-/-})$ mice, and all of these mice were on an AKR/J genetic background. We have established breeding colonies of these mice in-house. GPR30$(^{-/-})$ mice were healthy and fertile. Of special note is that the ERα$(^{+/-})$ heterozygotes were also fertile and showed no obvious phenotypes in association with the disrupted *Erα* genotype. A cross between heterozygous ERα$(^{+/-})$ mice resulted in the live birth of normal litter sizes of homozygous ERα$(^{-/-})$ mice. To generate GPR30$(^{-/-})$/ERα$(^{-/-})$ mice, we have made a cross between GPR30$(^{-/-})$ mice and heterozygous ERα$(^{+/-})$ mice to create GPR30$(^{-/-})$/ERα$(^{+/-})$ mice. After that, GPR30$(^{-/-})$/ERα$(^{+/-})$ mice were bred to generate female GPR30$(^{-/-})$/ERα$(^{-/-})$ mice for the studies.

To exclude possible interindividual differences in endogenous estrogen concentrations, all experimental animals were gonadectomized and subsequently implanted with 17β-estradiol (E_2)-releasing pellets (Innovative Research of America, Sarasota, FL). In brief, at 4 weeks of age, female mice were ovariectomized (OVX). At 8 weeks of age, the mice were implanted subcutaneously with pellets releasing E_2 at 0 or 6 µg/day for 12 days. All animals were maintained in a temperature-controlled room (22 ± 1°C) with a 12-h day cycle (lights on from 0600 h to 1800 h) and were provided free access to water and normal mouse chow containing trace cholesterol (<0.02%) (Lab Rodent Diet, St. Louis, MO). To dissect the lithogenic effects of GPR30 and ERα on cholesterol crystallization during the early stage of gallstone formation, mice at 8 weeks old were fed the lithogenic diet containing 1% cholesterol, 15% butter fat, and 0.5% cholic acid for 12 days. All procedures were in accordance with current National Institutes of Health guidelines and were approved by the Institutional Animal Care and Use Committee of Saint Louis University (St. Louis, MO).

Microscopic studies of cholesterol crystallization

After anesthetization with pentobarbital, a cholecystectomy was performed in overnight fasted mice (n = 5 per group for each time point) before (day 0, on chow) and at 3, 6, 9 and 12 days on the lithogenic diet. After a small hole was made in the fundus of the gallbladder, bulk bile dribbled by gravity, and mucin gels were pressed out digitally with the assistance of a 24 gauge needle. The entire gallbladder bile sample was placed on a glass slide at room temperature (∼22°C) and observed without a cover slip using a polarizing light microscope and then with a cover slip using phase contrast optics. These gallbladder bile samples were examined by microscopic analysis for the presence of mucin gels, liquid crystals, solid cholesterol monohydrate crystals, sandy stones, and real gallstones according to previously published criteria (16). Mucin gels were observed as nonbirefringent amorphous strands. Arc-like and tubular crystals (assumed to be metastable transitional forms of anhydrous cholesterol being hydrated to cholesterol monohydrate crystals), plate-like cholesterol monohydrate crystals, as well as small, aggregated, and fused liquid crystals were defined according to previously established criteria (17). The images of cholesterol monohydrate crystals were analyzed by a Carl Zeiss Imaging System with an AxioVision Rel 4.6 software (Carl Zeiss Microimaging, GmbH Göttingen, Germany). After microscopic analysis, gallbladder bile was collected, frozen, and stored at –20°C for lipid studies.

Biliary lipid analysis

Biliary cholesterol was determined using an enzymatic assay (18). Biliary phospholipids were measured as inorganic phosphorus by the method of Bartlett (19). Total bile salt concentration was measured enzymatically by the 3α-hydroxysteroid dehydrogenase method (20). Individual bile salt species were determined by HPLC (21). Cholesterol saturation index (CSI) of pooled gallbladder bile was calculated from critical tables (22) that were established for taurocholate, the predominant bile salt in bile of mice on the lithogenic diet. The hydrophobicity index of bile samples was calculated according to Heuman's method (23). Relative lipid compositions of pooled gallbladder bile (n = 5 per group at each time point) were plotted on condensed phased diagrams. For graphic analysis, the phase limits of the micellar zones and the crystallization pathways were extrapolated from model systems developed for taurocholate at 37°C and at a total lipid concentration of 9 g/l (17).

Dynamic measurement of gallbladder emptying function

At 12 days after E_2 treatment and the lithogenic diet feeding, a dynamic measurement of gallbladder emptying function was

performed in mice (n = 4 per group) in response to a high-fat meal according to previously published methods (24). After mice were fasted overnight but had free access to water, they were anesthetized with pentobarbital. During laparotomy, a PE-10 polyethylene catheter was inserted into the duodenum. The duodenal catheter was externalized through the left abdominal wall and connected to an infusion pump (Kent Scientific, Litchfield, CT). After all the surgical procedures were completed, the gallbladder was clearly exposed, and its volume was carefully measured with a micro-caliper. By assuming an ellipsoid shape of the organ, fasting gallbladder volume was calculated using the following formula: Gallbladder volume (μl) = length (mm) × width (mm) × depth (mm) × $\pi/6$.

To measure postprandial gallbladder volume, mice were intraduodenally infused with corn oil (i.e., a fatty meal) at 40 μl/min for 5 min. At 30 min after the corn oil infusion, gallbladder volume was carefully measured again with a micro-caliper. Gallbladder emptying function was calculated by a difference in gallbladder volume before and after the duodenal infusion of corn oil.

Immunohistochemistry

Representative blocks of paraffin-embedded gallbladder tissues were cut at 4 μm thickness, dewaxed, and rehydrated. For GPR30 and ERα staining, antigens were retrieved by boiling in 10 mM citrate buffer (pH 7.0) for 1 min. All the staining processes were performed by using a Histostain Plus 3rd Gen IHC Detection Kit according to the manufacturer's instructions (Invitrogen, Camarillo, CA). The sections were incubated with anti-GPR30 or anti-ERα antibodies (Santa Cruz, Dallas, TX) at a dilution of 1:100. The primary antibodies were replaced by the blocking solution containing 10% nonimmune goat serum for negative control slides. After washing, the sections were incubated with the corresponding secondary antibodies for 30 min at room temperature. Subsequently, the sections were counterstained with hematoxylin, dehydrated through an alcohol series to xylene, and mounted.

Quantitative real-time PCR assay

Total RNA was extracted from gallbladder tissues of mice (n = 4 per group) using RNeasy Mini (Qiagen, Valencia, CA). Reverse transcription reaction was performed using the iScript Reverse Transcription Supermix for quantitative RT-PCR (Bio-Rad, Hercules, CA) with 1 μg of total RNA and random hexamers to generate cDNA. Primer Express Software (Applied Biosystems, Foster City, CA) was used to design the primers based on sequence data available from GenBank. Supplementary Table 1 lists the sequences of the primers for the genes below. The mRNA levels of mucin gene 1 (*Muc1*), *Muc2*, *Muc3*, *Muc4*, *Muc5ac*, *Muc5b*, cholecystokinin-1 receptor (*Cck-1r*), acyl-CoA:cholesterol acyltransferase, isoform 2 (*Acat2*), scavenger receptor class B, member 1 (*Sr-b1*), ATP-binding cassette transporter g5 (*Abcg5*), *Abcg8*, and *Abca1* in the gallbladder were examined in triplicate by quantitative real-time PCR assays (25). Relative mRNA levels were calculated using the threshold cycle of an unknown sample against a standard curve with known copy numbers. To obtain a normalized target value, the target amount was divided by the endogenous reference amount of mouse β-*Actin* as internal control.

Statistical method

All data are expressed as mean ± SD. Statistically significant differences among groups of mice were assessed by Student's *t*-test, Mann-Whitney U-tests, or Chi-square tests. If the F-value was significant, comparisons among groups of mice were further analyzed by a multiple comparison test. Analyses were performed with SuperANOVA software (Abacus Concepts, Berkeley, CA). Statistical significance was defined as a two-tailed probability of less than 0.05.

RESULTS

### Effect of GPR30 and ERα on the morphology of liquid crystals and solid cholesterol crystals

As shown in **Fig. 1**, during the 12-day period of E_2 treatment and the lithogenic diet feeding, multiple types of cholesterol crystals formed in OVX GPR30($^{-/-}$) mice, with arc-like and tubular crystals of anhydrous cholesterol evolving to the classical notched rhombohedral cholesterol monohydrate crystals. By contrast, solid plate-like cholesterol monohydrate crystals precipitated from the liquid crystalline pathway in OVX ERα($^{-/-}$) mice. Both the anhydrous crystalline and the liquid crystalline habits were observed in OVX wild-type mice. However, no liquid crystals or solid cholesterol crystals were found in OVX GPR30($^{-/-}$)/ERα($^{-/-}$) mice. These results indicated that the activation of GPR30 by E_2 promoted the precipitation of solid cholesterol monohydrate crystals from liquid crystals independently of ERα because the latter induced cholesterol crystallization from the anhydrous crystalline pathway.

Effect of GPR30 and ERα on cholesterol crystallization sequences

Figure 2 illustrates cholesterol crystallization pathways and sequences in gallbladder bile of OVX mice treated with E_2 as functions of days on the lithogenic diet. In OVX wild-type mice, a thick layer of sticky mucin gels adherent to the gallbladder wall was first observed, followed by liquid crystals and anhydrous cholesterol crystals. At day 9, cholesterol monohydrate crystals were present with mucin
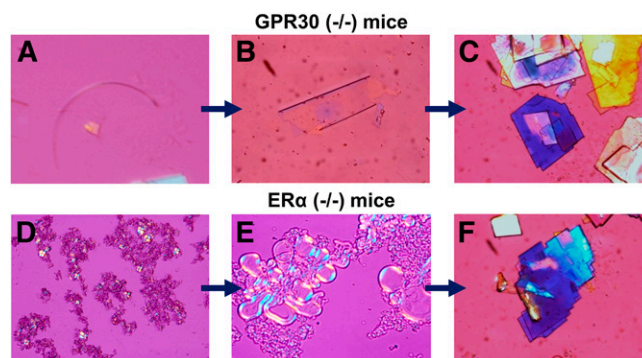
Fig. 1. Representative photomicrographs of two cholesterol crystallization pathways: the anhydrous crystalline pathway in OVX GPR30($^{-/-}$) mice and the liquid crystalline pathway in OVX ERα($^{-/-}$) mice during the 12-day period of E_2 (6 μg/day) treatment and the lithogenic diet feeding. A: Arc-like crystal. B: Tubular crystal. C: Solid plate-like cholesterol monohydrate crystals. D: Aggregated liquid crystals. E: Fused liquid crystals. F: Typical cholesterol monohydrate crystals. All magnifications are ×800 by polarizing light microscopy.
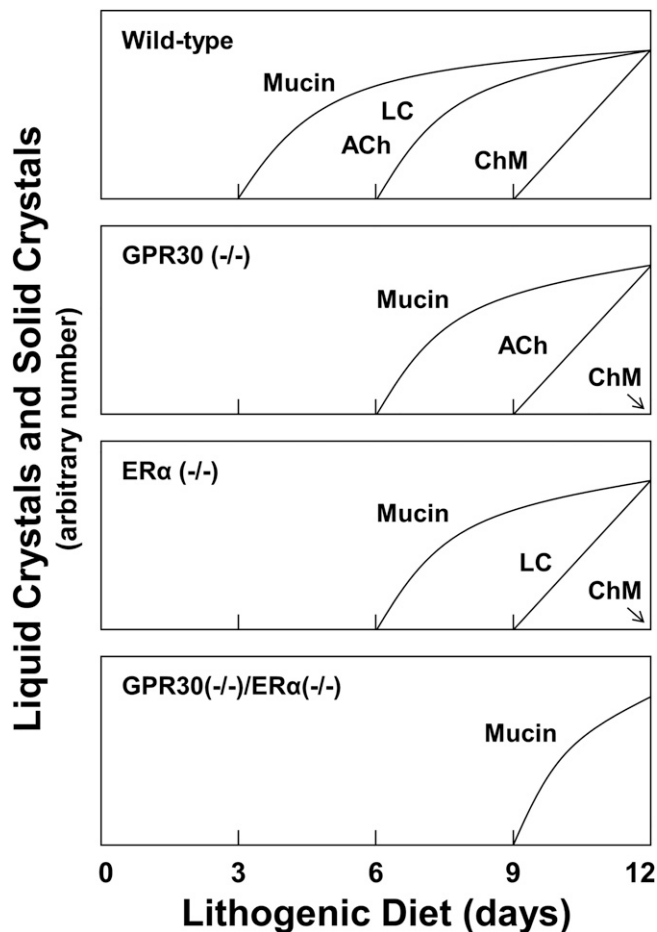
Fig. 2. Schematic presentation of the crystal habits in cholesterol crystallization sequences from gallbladder bile as functions of days on the lithogenic diet in OVX mice treated with E_2 at 6 μg/day for 12 days. The vertical axes represent arbitrary numbers of liquid crystals and solid crystals per high-power microscopic field, with all being normalized to the same maximum. The panels show the time sequences for OVX wild-type, GPR30($^{-/-}$), ERα($^{-/-}$), and GPR30($^{-/-}$)/ERα($^{-/-}$) mice. Abbreviations: ACh, anhydrous cholesterol crystals, including arc-like and transitional tubular crystals; ChM, classical plate-like cholesterol monohydrate crystals; LC, liquid crystals, including small, aggregated, and fused (multilamellar) varieties.

gels. At day 12, solid cholesterol monohydrate crystals were consolidated by mucin gels as agglomerates. In OVX GPR30($^{-/-}$) mice, mucin gels appeared first, followed by anhydrous cholesterol crystals and then cholesterol monohydrate crystals. As expected, mucin gels appeared first in OVX ERα($^{-/-}$) mice. Subsequently, aggregated and fused liquid crystals were found at day 9, and many cholesterol monohydrate crystals precipitated in bile at day 12. We found that after 12 days on the lithogenic diet, the number of solid cholesterol monohydrate crystals was markedly greater in OVX wild-type mice than in OVX GPR30($^{-/-}$) and ERα($^{-/-}$) mice. Notably, only a thin layer of mucin gels appeared at day 9 in OVX GPR30($^{-/-}$)/ERα($^{-/-}$) mice. No liquid crystals or solid cholesterol crystals were detected in these mice at 12 days. These results indicated that the time of cholesterol crystallization was greatly prolonged in OVX GPR30($^{-/-}$)/ERα($^{-/-}$) mice.

Phase analysis of gallbladder bile during cholesterol crystallization

Table 1 lists the relative biliary lipid compositions of pooled gallbladder bile in OVX mice treated with E_2 as well as before (day 0, on chow) and during feeding the lithogenic diet for 12 days. For phase analysis, a group of truncated phase diagrams was created for pooled gallbladder bile of OVX mice during the 12-day period of E_2 treatment and the lithogenic diet feeding (**Fig. 3**). In the lithogenic state, relative lipid compositions of pooled gallbladder bile gradually moved upward and to the right of the phase diagrams in all groups of OVX mice. Such a shift was caused by a relative increase in cholesterol and phospholipid concentrations and a relative decrease in bile salt concentrations. In OVX wild-type mice, relative biliary lipid compositions of bile at day 0 and day 3 were located within the micellar zone, whereas after day 6, relative biliary lipid compositions passed through region B and entered region C. By phase analysis, the bile was composed of two or three phases, namely saturated micelles, solid cholesterol crystals, or plus liquid crystals. In OVX GPR30($^{-/-}$) mice, relative biliary lipid compositions of bile at day 9 entered region B, in which arc-like and tubular crystals appeared before cholesterol monohydrate crystals. During lithogenesis, relative lipid compositions of bile in OVX ERα($^{-/-}$) mice directly entered region C from the micellar zone. As expected, liquid crystals invariably preceded cholesterol monohydrate crystals during crystallization. Of note, relative biliary lipid composition of bile in OVX GPR30($^{-/-}$)/ERα($^{-/-}$) mice still stayed in the micellar zone. By phase analysis, the bile consisted of only unsaturated micelles, indicating that gallbladder bile was unsaturated.

Effect of GPR30 and ERα on bile salt species in gallbladder bile

Analysis of individual bile salt species by HPLC showed that all bile salts in gallbladder bile of E_2-treated mice were taurine conjugated with a similar distribution of bile salt composition. As expected, in these mice fed the lithogenic diet, taurocholate (50.5–55.5%) was the major bile salt of biliary pool, followed by taurochenodeoxycholate (13.3–32.4%). There was a low concentration in tauro-β-muricholate (4.5–13.9%), taurodeoxycholate (6.0–9.6%), tauro-ω-muricholate (0.9–7.2%), and tauroursodeoxycholate (3.2–5.5%). Hydrophobicity indexes of bile salts in bile were comparable (–0.08 to +0.14) among four groups of mice. These results indicate that the deletion of either the *Erα* or the *Gpr30* gene alone, or both did not influence bile salt species in bile.

Effect of GPR30 and ERα on gallbladder motility function

At 12 days on the lithogenic diet, E_2 treatment caused the largest fasting gallbladder volumes in OVX wild-type mice, followed by OVX GPR30($^{-/-}$), ERα($^{-/-}$), and GPR30($^{-/-}$)/ERα($^{-/-}$) mice (**Fig. 4**). We also measured postprandial gallbladder volumes in these mice in response to a fatty meal. We observed that a significant portion of

TABLE 1. Biliary lipid compositions of pooled gallbladder bile during cholesterol crystallization

Day	Ch (mol%)	PL (mol%)	BS (mol%)	Ch/PL Ratio	Ch/BS Ratio	[TL] (g/dl)	CSI
Wild-type							
0	2.47	11.50	86.03	0.215	0.029	8.94	0.56
3	3.28	12.68	84.03	0.259	0.039	8.77	0.70
6	5.03	13.31	81.66	0.378	0.062	9.45	1.01
9	5.74	15.15	79.12	0.379	0.073	9.46	1.05
12	6.83	16.27	76.91	0.420	0.089	9.84	1.17
GPR30($^{-/-}$)							
0	1.98	10.68	87.34	0.185	0.023	8.76	0.47
3	2.29	13.05	84.66	0.175	0.027	8.69	0.48
6	3.56	14.27	82.17	0.250	0.043	8.67	0.70
9	5.16	13.96	80.88	0.370	0.064	8.81	1.01
12	6.10	15.77	78.13	0.387	0.078	10.48	1.06
ERα($^{-/-}$)							
0	1.87	10.68	87.45	0.175	0.021	8.82	0.44
3	2.54	13.00	84.47	0.195	0.030	8.94	0.53
6	3.54	13.14	83.32	0.269	0.042	8.73	0.73
9	5.52	16.08	78.39	0.343	0.070	8.04	1.00
12	5.94	16.20	77.86	0.367	0.076	9.86	1.02
GPR30($^{-/-}$)/ERα($^{-/-}$)							
0	1.55	11.35	87.09	0.137	0.018	8.22	0.36
3	2.19	12.06	85.75	0.181	0.025	8.47	0.49
6	2.78	15.05	82.17	0.184	0.034	8.35	0.53
9	3.39	15.91	80.70	0.213	0.042	8.49	0.62
12	4.09	17.45	78.46	0.234	0.052	9.26	0.69

Values were determined from pooled gallbladder bile (n = 5 per group). BS, bile salts; Ch, cholesterol; CSI, cholesterol saturation index; PL, phospholipids; [TL], total lipid concentration.

gallbladder bile was emptied out in OVX GPR30($^{-/-}$)/ERα($^{-/-}$) mice in response to the fatty meal. However, it was not the case in OVX wild-type, GPR30($^{-/-}$), and ERα($^{-/-}$) mice, suggesting an impaired gallbladder emptying function in these mice.

Effect of GPR30 and ERα on growth patterns of solid cholesterol crystals

Bile stasis induced by hypomobile gallbladder provides the time necessary to accommodate growth and agglomeration of solid cholesterol crystals into microlithiasis entrapped within mucin gels. Therefore, gallbladder hypomotility is an important risk factor for gallstone formation (26). **Figure 5** displays three modes of growth habits of solid cholesterol crystals, as observed in E$_2$-treated OVX wild-type mice with the highest CSI value. Figure 5A shows the most common crystal growth habit: proportional enlargement patterns in which solid cholesterol crystals grow bidirectionally (i.e., by both length and width). The second mode of crystal growth habit was spiral dislocation growth, with the pyramidal surface containing numerous spiral layers crystallizing by a screw dislocation (Fig. 5B). The third mode of crystal growth habit was twin crystal growth, with the crystals growing upright and perpendicular to the surface (Fig. 5C). All of these crystal growth habits led to a rapid enlargement of solid cholesterol crystals in size.

## Detection of GPR30 and ERα in the gallbladder by Immunohistochemistry

As revealed by immunohistochemical studies (**Fig. 6**), GPR30 was expressed in the epithelial and smooth muscle cells of gallbladder, and it is present predominantly in the former, whereas ERα was expressed mainly in the gallbladder smooth muscle cells in chow-fed female wild-type

mice with intact ovaries. Furthermore, in chow-fed female ERα($^{-/-}$) mice with intact ovaries, the presence of ERα was not detected, but the staining for GPR30 was clearly observed in the gallbladder (data not shown). In chow-fed female GPR30($^{-/-}$) mice with intact ovaries, ERα, but not GPR30, expression was found in the gallbladder. Moreover, no GPR30 or ERα expression was detected in the gallbladder of chow-fed female GPR30($^{-/-}$)/ERα($^{-/-}$) mice with intact ovaries.

Effect of GPR30 and ERα on expression of gallbladder estrogen receptor and mucin genes, and the genes involved in lipid transport and metabolism, and gallbladder motility

In the lithogenic state, mRNA levels of *Erα* in the gallbladder were significantly increased in OVX wild-type and GPR30($^{-/-}$) mice treated with E$_2$ at 6 μg/day compared with OVX wild-type mice receiving no E$_2$ (**Fig. 7**). As expected, the absence in expression of *Erα* in the gallbladder confirms its complete knockout in OVX ERα($^{-/-}$) and GPR30($^{-/-}$)/ERα($^{-/-}$) mice. In the gallbladder, expression of *Erβ* is very low, and its expression is comparable among these groups of OVX mice. Moreover, mRNA levels of *Gpr30* in the gallbladder were increased in OVX wild-type and ERα($^{-/-}$) mice. However, the difference did not reach statistical significance. Again, the absence of *Gpr30* expression in the gallbladder confirms its complete knockout in OVX GPR30($^{-/-}$) and GPR30($^{-/-}$)/ERα($^{-/-}$) mice.

As shown in **Fig. 8**, at 12 days on the lithogenic diet, E$_2$ treatment significantly increased mRNA levels of *Muc2*, *Muc5ac*, and *Muc5b* (for producing the gel-forming mucins) but not *Muc1*, *Muc3*, and *Muc4* (for producing the epithelial mucins) in OVX wild-type, GPR30($^{-/-}$), and ERα($^{-/-}$) mice compared with those in OVX wild-type

A Wild-type

**B GPR30 (-/-)**

C ERα (-/-)

D GPR30(-/-)/ERα(-/-)
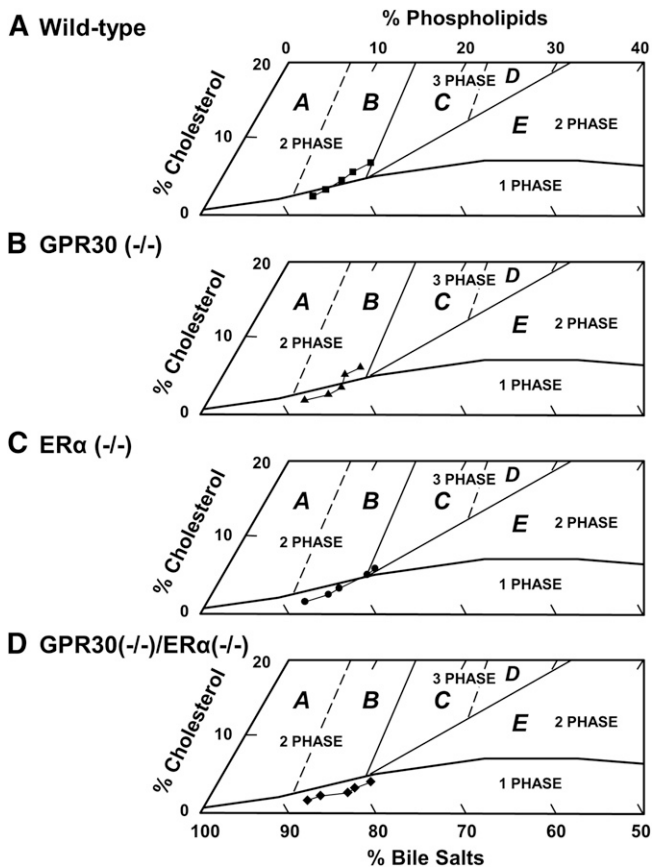
Fig. 3. The relative lipid compositions (mol per 100 mol) of pooled gallbladder bile (n = 5 per group) at each time point (0, 3, 6, 9, and 12 days on the lithogenic diet) are plotted on condensed phase diagrams. The one-phase micellar zone at the bottom is enclosed by a solid curved line. Above the micellar zone, two solid and two dashed lines divide the phase diagrams into regions A to E with different crystallization sequences (17). With passage of time, relative biliary lipid compositions of pooled gallbladder bile progressively move upward and to the right in (A) OVX wild-type, (B) GPR30($^{-/-}$), (C) ERα($^{-/-}$), and (D) GPR30($^{-/-}$)/ERα($^{-/-}$) mice during the 12-day period of E_2 treatment and the lithogenic diet feeding. However, they either stay in the micellar zone or enter different regions for cholesterol crystallization.

mice receiving no E_2. Moreover, mRNA levels of *Abcg5*, *Abcg8*, *Abca1*, *Sr-b1* (the gallbladder lipid transporters), and *Acat2* (for cholesterol esterification) were significantly increased in OVX wild-type, GPR30($^{-/-}$), and ERα($^{-/-}$) mice. By contrast, mRNA levels of *Cck-1r* were significantly reduced in OVX wild-type and GPR30($^{-/-}$) mice fed the lithogenic diet for 12 days. Notably, expression of the genes described above was comparable in OVX GPR30($^{-/-}$)/ERα($^{-/-}$) mice compared with that in OVX wild-type mice receiving no E_2.

DISCUSSION

Recent progress in understanding the molecular biological basis of GPR30, ERα, and ERβ has provided many novel insights into the complex pathophysiological mechanisms underlying the lithogenic effect of E_2 on cholesterol
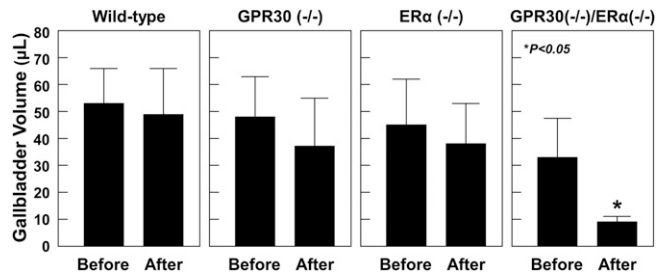
Fig. 4. Postprandial gallbladder volumes in response to a fatty meal in OVX mice treated with E_2 and fed the lithogenic diet for 12 days. Duodenal infusion of corn oil stimulates the release of CCK from the upper part of the small intestine. As a result, the secreted CCK induces gallbladder emptying in GPR30($^{-/-}$)/ERα($^{-/-}$) mice but not in OVX wild-type, GPR30($^{-/-}$), and OVX ERα($^{-/-}$) mice, indicating that gallbladder contractile function is impaired in the latter three groups of mice.

crystallization and gallstone formation (11). In the present study, the most important findings are that (i) E_2 disrupts biliary cholesterol and bile salt homeostasis through ERα and GPR30, leading to a distinctly abnormal metastable physical-chemical state of bile predisposing to supersaturation with cholesterol; (ii) E_2 activates GPR30 and ERα to produce liquid crystalline versus anhydrous crystalline metastable intermediates evolving to solid plate-like cholesterol monohydrate crystals in supersaturated bile; and (iii) GPR30 produces a synergistic lithogenic action with ERα to promote E_2-induced gallstone formation.

We found that upon feeding the lithogenic diet, an early onset of cholesterol-supersaturated gallbladder bile, as well as rapid cholesterol crystallization and crystal growth, occur in OVX wild-type mice, followed by OVX GPR30($^{-/-}$) and ERα($^{-/-}$) mice. Of note, we have found that the activation of GPR30 by E_2 results in markedly lower hepatic bile salt output in OVX ERα($^{-/-}$) mice, suggesting a reduction in hepatic synthesis and biliary output of bile salts (11). By contrast, the activation of ERα by E_2 leads to markedly higher hepatic cholesterol output in OVX GPR30($^{-/-}$) mice, suggesting an increase in hepatic cholesterol synthesis. These results are consistent with our early findings that E_2 inhibits the negative feedback regulation of cholesterol synthesis determined by the SREBP-2 signaling pathway through the hepatic ERα (25). Therefore, under E_2 treatment, there is a continuous cholesterol synthesis in the liver for biliary hypersecretion. The phase analysis of pooled gallbladder bile reveals that in the early stage of cholesterol crystallization, relative lipid compositions of bile in OVX GPR30($^{-/-}$) and ERα($^{-/-}$) mice enter regions B and C from the micellar zone, respectively. Moreover, relative lipid compositions of bile in OVX wild-type mice enter region C by passing through region B. By contrast, relative lipid compositions of bile in OVX GPR30($^{-/-}$)/ERα($^{-/-}$) mice still stay in the one-phase micellar zone, indicating that bile is unsaturated and does to form solid cholesterol crystals or liquid crystals. Many clinical studies have found that patients with cholesterol gallstones who are exposed to oral contraceptive steroids and
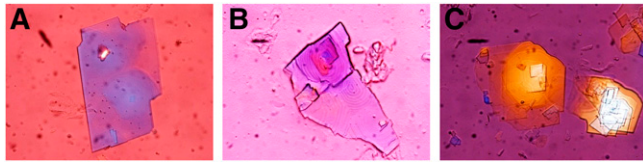
Fig. 5. Three modes of cholesterol crystal growth habits in OVX wild-type mice. Proportional enlargement pattern (A), spiral dislocation growth pattern (B), and twin crystal growth pattern (C), all of which enlarge the size of solid cholesterol crystals. All magnifications are ×800 by polarizing light microscopy.

conjugated estrogens demonstrate two types of biliary cholesterol hypersecretion (i.e., relative high hepatic cholesterol output is accompanied by either normal or low hepatic bile salt output) (3, 27–29). This implies that these clinical features may be attributable to the differences between GPR30 and ERα in varying responses to high levels of E_2. Our findings indicate, therefore, that the activation of GPR30 and ERα by E_2 accelerates cholesterol crystallization through two distinct crystallization mechanisms (i.e., the liquid crystalline and the anhydrous crystalline pathways evolving to classical plate-like cholesterol monohydrate crystals).

It has been recognized that the gallbladder also plays a critical role in the pathogenesis of gallstone formation because increased fasting gallbladder volume, together with impaired postprandial and interdigestive gallbladder emptying, are frequent and distinctive features in patients with cholesterol gallstones (26, 30). Thus, gallbladder stasis provides time for the nucleation and crystallization of solid cholesterol crystals and their growth and agglomeration into microlithiasis. The gallbladder epithelial cells have a role in actively modifying the lipid compositions of bile by secretion and absorption of lipids and water (31).
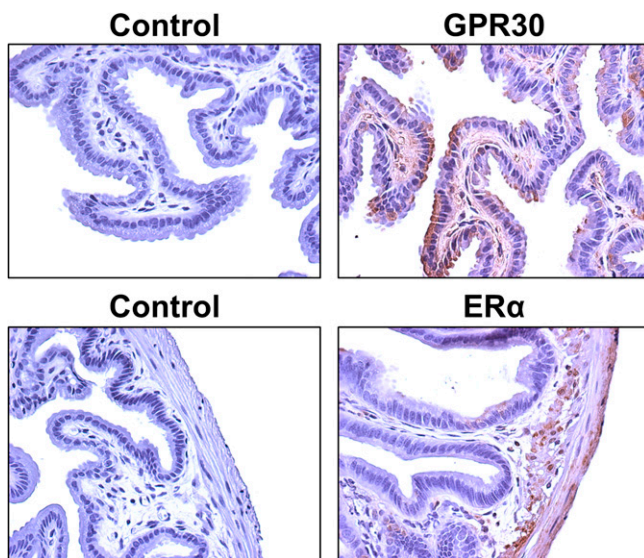

Fig. 6. Immunohistochemical studies reveal that GPR30 is expressed in the epithelial cells and smooth muscle cells of the gallbladder, and it is present predominantly in the former. By contrast, ERα is expressed mainly in the gallbladder smooth muscle cells. All magnifications are ×400.

In the lithogenic state, gallbladder stasis promotes partitioning of cholesterol monomers out of saturated micelles for gallbladder absorption by cholesterol influx transporters on the apical membrane of the gallbladder epithelial cells. We found that E_2 treatment increased mRNA levels of *Abcg5*, *Abcg8*, *Abca1*, and *Sr-b1*, which encode the cholesterol transporters in the gallbladder epithelial cells, in OVX wild-type, GPR30($^{-/-}$), and ERα($^{-/-}$) mice but not in GPR30($^{-/-}$)/ERα($^{-/-}$) mice. These abnormalities could lead to an imbalance between influx and efflux of cholesterol in the gallbladder epithelial cells. Because GPR30 and ERα are localized in the endoplasmic reticulum and the nucleus of cells, respectively (32), GPR30 may regulate the expression of target genes by a nontranscriptional regulatory mode through the epidermal growth factor receptor signaling cascade in response to E_2. By contrast, ERα regulates the expression of target genes by a transcriptional mechanism. Obviously, further studies are needed to investigate whether GPR30 and ERα mediates activities of these gallbladder sterol transporters through these two distinct regulatory mechanisms to enhance influx of intraluminal cholesterol molecules across the apical membrane of the epithelial cells.

Supersaturated bile further facilitates gallbladder cholesterol absorption and the accumulation of excess cholesterol in the gallbladder wall. Consequently, the enhanced gallbladder cholesterol absorption induces an increase in expression of *Acat2* in E_2-treated mice. The absorbed cholesterol has to be converted to cholesteryl esters for storage in the mucosa and lamina propria because gallbladder epithelial cells apparently cannot synthesize lipoproteins for lipid transport into the circulation. Thus, excess cholesterol in smooth muscle cells could stiffen sarcolemmal membranes and decouple the G-protein-mediated signal transduction, paralyzing gallbladder contractile function and impairing gallbladder emptying (33). Indeed, expression of *Cck-1r* in the gallbladder is reduced in OVX wild-type and GPR30($^{-/-}$) mice. This may be attributable, in part, to the impairment of gallbladder contractile function. The mRNA levels of *Cck-1r* are low in OVX ERα($^{-/-}$) mice but without statistical significance. Moreover, the lithogenic effect of E_2 on gallbladder motility function is blocked in OVX mice with the disruption of both the *Gpr30* and *Erα* genes. As revealed by immunohistochemical studies, although GPR30 is expressed in the epithelial cells and smooth muscle cells of the gallbladder, it is present mainly in the former. By contrast, ERα is expressed predominantly in the gallbladder muscle cells. These findings suggest that GPR30 may have a main effect in enhancing gallbladder cholesterol absorption by disrupting the function of gallbladder sterol transporters in the epithelial cells and that ERα may play a pivotal role in inhibiting the expression of cholecystokinin-1 receptor (CCK-1R) in the muscle cells for inducing gallbladder stasis. As a result, GPR30 and ERα impair gallbladder motility function possibly through different mechanisms in response to high levels of E_2.

It is well known that mucin hypersecretion and accumulation in the gallbladder is a prerequisite for gallstone
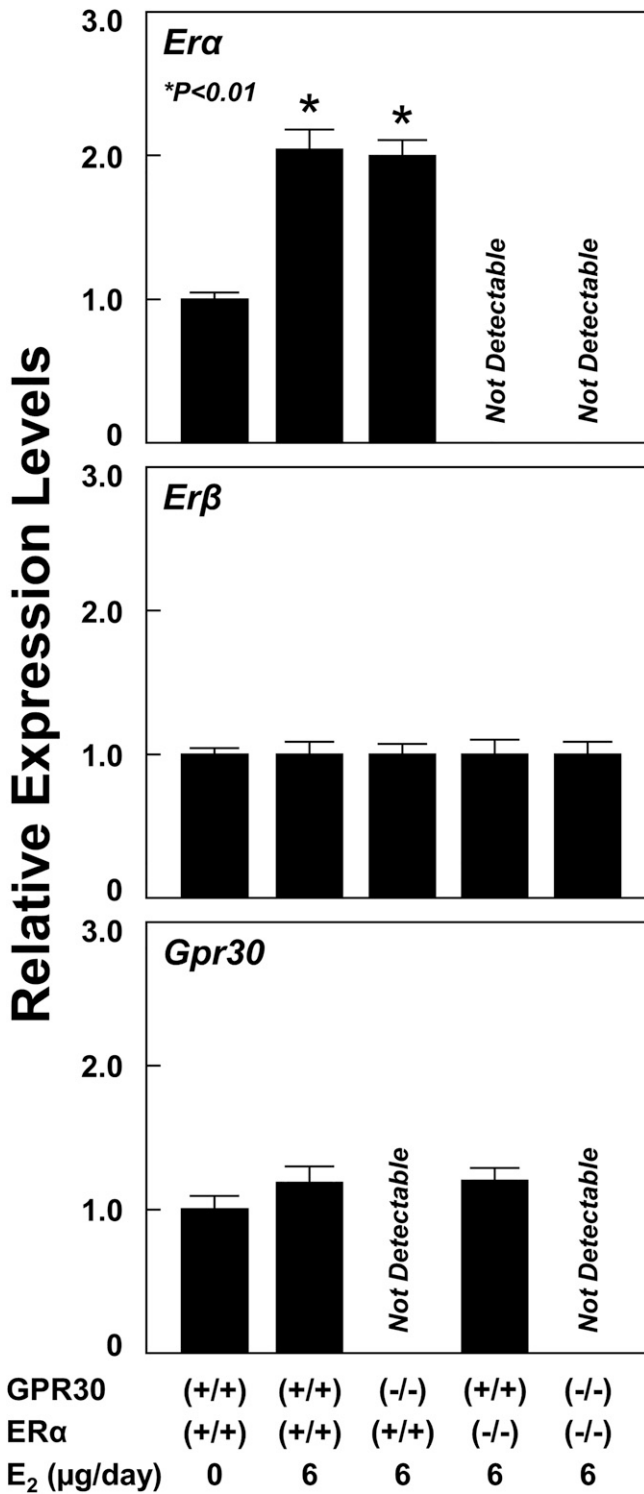
Fig. 7. Effect of E$_2$ on the expression of the *Erα*, *Erβ*, and *Gpr30* genes in the gallbladder. The data are expressed relative to mRNA levels of *Erα*, *Erβ*, and *Gpr30* in the gallbladder of OVX wild-type mice treated with E$_2$ at 0 or 6 µg/day and fed the lithogenic diet for 12 days, and their relative expression levels are set at 1. Treatment of E$_2$ at 6 µg/day results in a significant increase in mRNA levels of the gallbladder *Erα* but not *Erβ* or *Gpr30* genes in OVX wild-type and GPR30($^{-/-}$) mice. Notably, expression of *Erβ* and *Gpr30* is low in the gallbladder. The absence of *Erα* and *Gpr30* expression in the gallbladder confirms their complete knockout in OVX ERα($^{-/-}$), GPR30($^{-/-}$), and GPR30($^{-/-}$)/ERα($^{-/-}$) mice, respectively. See text for details.
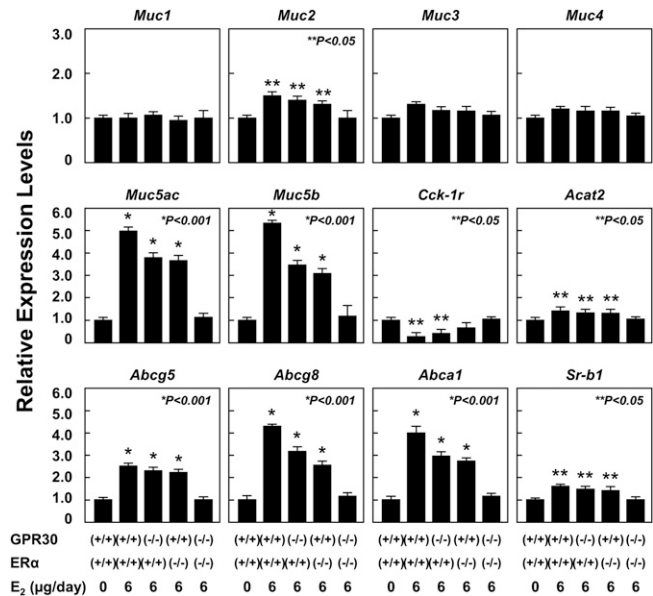
Fig. 8. Effect of E$_2$ on mRNA levels of gallbladder mucin genes as well as the genes involved in lipid transport and metabolism, and gallbladder motility in OVX wild-type, GPR30($^{-/-}$), ERα($^{-/-}$), and GPR30($^{-/-}$)/ERα($^{-/-}$) mice treated with E$_2$ at 0 or 6 µg/day and fed the lithogenic diet for 12 days. The mRNA levels of these genes in OVX wild-type mice receiving no E$_2$ and fed the lithogenic diet for 12 days are set at 1. Treatment of E$_2$ at 6 µg/day significantly increases mRNA levels of *Muc2*, *Muc5ac*, *Muc5b*, *Acat2*, *Abcg5*, *Abcg8*, *Abca1*, and *Sr-b1* in OVX wild-type, GPR30($^{-/-}$), and ERα($^{-/-}$), but not GPR30($^{-/-}$)/ERα($^{-/-}$) mice. However, expression of *Cck-1r* is significantly reduced in OVX wild-type and GPR30($^{-/-}$) but not ERα($^{-/-}$) or GPR30($^{-/-}$)/ERα($^{-/-}$) mice. Notably, expression of *Muc1*, *Muc3*, and *Muc4* in the gallbladder is comparable in the five groups of mice. See text for further description and for abbreviations.

formation (26). Increased amounts of gallbladder mucins are consistently observed in gallbladder bile of humans and of several animal models of cholesterol gallstones (34). Mucin synthesis and secretion in the gallbladder is determined by multiple mucin genes (35). Gallbladder mucins, a heterogeneous family of *O*-linked glycoproteins, are divided into two classes: the gel-forming and the epithelial mucins. The gel-forming mucins encoded by *Muc2*, *Muc5ac*, and *Muc5b* provide a protective coating to the underlying mucosa and form disulfide-stabilized oligo- or polymers, a phenomenon that accounts for their viscoelastic properties (36, 37). Accumulated evidence from native and model bile studies found that gallbladder gel-forming mucins are a potent pro-crystallizing agent for accelerating cholesterol crystallization (38). Moreover, the epithelial mucins produced by *Muc1*, *Muc3*, and *Muc4* are integral membrane glycoproteins located on the apical surface of epithelial cells and do not form aggregates (37). Their expression in the gallbladder is comparable in these four groups of mice even when treated with E$_2$ for 12 days. These results indicate that in the lithogenic state, E$_2$ promotes hypersecretion and accumulation of the gel-forming, but not the epithelial, mucins in the gallbladder mainly through ERα.

We have reported that abnormal gallbladder motility promotes not only the crystallization and precipitation of

solid cholesterol crystals but also the crystal growth in bile of CCK($^{-/-}$) and CCK-1R($^{-/-}$) mice fed the lithogenic diet (24, 39). In the present study, we found that gallbladder contractile dysfunction caused by E$_2$ also promotes rapid growth of solid cholesterol crystals mainly in E$_2$-treated OVX wild-type mice with the highest CSI value. These observations on cholesterol crystal growth habits are consistent with those reported previously in model bile systems by Toor and colleagues (40) and in CCK($^{-/-}$) mice with gallbladder hypomotility (24).

In summary, the physical-chemical phenotypes of GPR30 and ERα in gallbladder bile described in the present study are crucial for elucidating the lithogenic mechanisms of E$_2$ during the early stage of cholesterol gallstone formation. This study therefore provides the connection between two major estrogen receptors (GPR30 and ERα) and cholesterol crystallization in mice in response to high levels of E$_2$ and constitutes the basic framework for studying how E$_2$ influences the cholesterol and bile salt metabolism in the liver and bile. Our findings also support the novel concept that GPR30 is involved in E$_2$-dependent lithogenic actions, working independently of ERα, because both GPR30 and ERα can work through different pathways to promote E$_2$-induced cholesterol crystallization. Furthermore, GPR30 produces a synergistic lithogenic effect with ERα on the formation of E$_2$-induced gallstones. Translational studies are urgently required to confirm that similar cholesterol crystallization pathways also occur in human cholelithogenesis during the early stage of gallstone formation and to identify better measures for preventing E$_2$-induced gallstone formation.

REFERENCES

1. Wang, D. Q., D. E. Cohen, and M. C. Carey. 2009. Biliary lipids and cholesterol gallstone disease. *J. Lipid Res.* **50(Suppl):** S406–S411.
2. Everhart, J. E., M. Khare, M. Hill, and K. R. Maurer. 1999. Prevalence and ethnic differences in gallbladder disease in the United States. *Gastroenterology.* **117:** 632–639.
3. Everson, G. T., C. McKinley, and F. Kern, Jr. 1991. Mechanisms of gallstone formation in women. Effects of exogenous estrogen (Premarin) and dietary cholesterol on hepatic lipid metabolism. *J. Clin. Invest.* **87:** 237–246.
4. Cirillo, D. J., R. B. Wallace, R. J. Rodabough, P. Greenland, A. Z. LaCroix, M. C. Limacher, and J. C. Larson. 2005. Effect of estrogen therapy on gallbladder disease. *JAMA.* **293:** 330–339.
5. Thijs, C., and P. Knipschild. 1993. Oral contraceptives and the risk of gallbladder disease: a meta-analysis. *Am. J. Public Health.* **83:** 1113–1120.
6. de Bari, O., T. Y. Wang, M. Liu, C. N. Paik, P. Portincasa, and D. Q. Wang. 2014. Cholesterol cholelithiasis in pregnant women: pathogenesis, prevention and treatment. *Ann. Hepatol.* **13:** 728–745.
7. Henriksson, P., K. Einarsson, A. Eriksson, U. Kelter, and B. Angelin. 1989. Estrogen-induced gallstone formation in males. Relation to changes in serum and biliary lipids during hormonal treatment of prostatic carcinoma. *J. Clin. Invest.* **84:** 811–816.
8. Angelin, B., H. Olivecrona, E. Reihner, M. Rudling, D. Stahlberg, M. Eriksson, S. Ewerth, P. Henriksson, and K. Einarsson. 1992. Hepatic cholesterol metabolism in estrogen-treated men. *Gastroenterology.* **103:** 1657–1663.
9. de Bari, O., H. H. Wang, P. Portincasa, C. N. Paik, M. Liu, and D. Q. Wang. 2014. Ezetimibe prevents the formation of oestrogen-induced cholesterol gallstones in mice. *Eur. J. Clin. Invest.* **44:** 1159–1168.
10. Wang, H. H., N. H. Afdhal, and D. Q. Wang. 2004. Estrogen receptor α, but not β, plays a major role in 17β-estradiol-induced murine cholesterol gallstones. *Gastroenterology.* **127:** 239–249.
11. Wang, H. H., M. Liu, D. J. Clegg, P. Portincasa, and D. Q. Wang. 2009. New insights into the molecular mechanisms underlying effects of estrogen on cholesterol gallstone formation. *Biochim. Biophys. Acta.* **1791:** 1037–1047.
12. Carmeci, C., D. A. Thompson, H. Z. Ring, U. Francke, and R. J. Weigel. 1997. Identification of a gene (GPR30) with homology to the G-protein-coupled receptor superfamily associated with estrogen receptor expression in breast cancer. *Genomics.* **45:** 607–617.
13. Lyons, M. A., R. Korstanje, R. Li, S. M. Sheehan, K. A. Walsh, J. A. Rollins, M. C. Carey, B. Paigen, and G. A. Churchill. 2005. Single and interacting QTLs for cholesterol gallstones revealed in an intercross between mouse strains NZB and SM. *Mamm. Genome.* **16:** 152–163.
14. Lyons, M. A., and H. Wittenburg. 2006. Cholesterol gallstone susceptibility loci: a mouse map, candidate gene evaluation, and guide to human *LITH* genes. *Gastroenterology.* **131:** 1943–1970.
15. Wang, H. H., P. Portincasa, N. H. Afdhal, and D. Q. Wang. 2010. *Lith* genes and genetic analysis of cholesterol gallstone formation. *Gastroenterol. Clin. North Am.* **39:** 185–207 (vii–viii.).
16. Wang, D. Q., B. Paigen, and M. C. Carey. 1997. Phenotypic characterization of *Lith* genes that determine susceptibility to cholesterol cholelithiasis in inbred mice: physical-chemistry of gallbladder bile. *J. Lipid Res.* **38:** 1395–1411.
17. Wang, D. Q., and M. C. Carey. 1996. Complete mapping of crystallization pathways during cholesterol precipitation from model bile: influence of physical-chemical variables of pathophysiologic relevance and identification of a stable liquid crystalline state in cold, dilute and hydrophilic bile salt-containing systems. *J. Lipid Res.* **37:** 606–630.
18. Fromm, H., P. Amin, H. Klein, and I. Kupke. 1980. Use of a simple enzymatic assay for cholesterol analysis in human bile. *J. Lipid Res.* **21:** 259–261.
19. Bartlett, G. R. 1959. Phosphorus assay in column chromatography. *J. Biol. Chem.* **234:** 466–468.
20. Turley, S. D., and J. M. Dietschy. 1978. Re-evaluation of the 3 alpha-hydroxysteroid dehydrogenase assay for total bile acids in bile. *J. Lipid Res.* **19:** 924–928.
21. Rossi, S. S., J. L. Converse, and A. F. Hofmann. 1987. High pressure liquid chromatographic analysis of conjugated bile acids in human bile: simultaneous resolution of sulfated and unsulfated lithocholyl amidates and the common conjugated bile acids. *J. Lipid Res.* **28:** 589–595.
22. Carey, M. C. 1978. Critical tables for calculating the cholesterol saturation of native bile. *J. Lipid Res.* **19:** 945–955.
23. Heuman, D. M. 1989. Quantitative estimation of the hydrophilic-hydrophobic balance of mixed bile salt solutions. *J. Lipid Res.* **30:** 719–730.
24. Wang, H. H., P. Portincasa, M. Liu, P. Tso, L. C. Samuelson, and D. Q. Wang. 2010. Effect of gallbladder hypomotility on cholesterol crystallization and growth in CCK-deficient mice. *Biochim. Biophys. Acta.* **1801:** 138–146.
25. Wang, H. H., N. H. Afdhal, and D. Q. Wang. 2006. Overexpression of estrogen receptor alpha increases hepatic cholesterogenesis, leading to biliary hypersecretion in mice. *J. Lipid Res.* **47:** 778–786.
26. Portincasa, P., A. Di Ciaula, H. H. Wang, G. Palasciano, K. J. van Erpecum, A. Moschetta, and D. Q. Wang. 2008. Coordinate regulation of gallbladder motor function in the gut-liver axis. *Hepatology.* **47:** 2112–2126.
27. Bennion, L. J., D. M. Mott, and B. V. Howard. 1980. Oral contraceptives raise the cholesterol saturation of bile by increasing biliary cholesterol secretion. *Metabolism.* **29:** 18–22.
28. Bennion, L. J., R. L. Ginsberg, M. B. Gernick, and P. H. Bennett. 1976. Effects of oral contraceptives on the gallbladder bile of normal women. *N. Engl. J. Med.* **294:** 189–192.
29. Angelin, B., H. Olivecrona, E. Reihner, M. Rudling, D. Stahlberg, M. Eriksson, S. Ewerth, P. Henriksson, and K. Einarsson. 1992. Hepatic cholesterol metabolism in estrogen-treated men. *Gastroenterology.* **103:** 1657–1663.
30. Portincasa, P., A. Moschetta, and G. Palasciano. 2006. Cholesterol gallstone disease. *Lancet.* **368:** 230–239.
31. van Erpecum, K. J., D. Q. Wang, F. Lammert, B. Paigen, A. K. Groen, and M. C. Carey. 2001. Phenotypic characterization of *Lith*

genes that determine susceptibility to cholesterol cholelithiasis in inbred mice: soluble pronucleating proteins in gallbladder and hepatic biles. *J. Hepatol.* **35:** 444–451.

32. Revankar, C. M., D. F. Cimino, L. A. Sklar, J. B. Arterburn, and E. R. Prossnitz. 2005. A transmembrane intracellular estrogen receptor mediates rapid cell signaling. *Science.* **307:** 1625–1630.

33. Xiao, Z. L., Q. Chen, J. Amaral, P. Biancani, R. T. Jensen, and J. Behar. 1999. CCK receptor dysfunction in muscle membranes from human gallbladders with cholesterol stones. *Am. J. Physiol.* **276:** G1401–G1407.

34. Lee, S. P., J. T. LaMont, and M. C. Carey. 1981. Role of gallbladder mucus hypersecretion in the evolution of cholesterol gallstones. *J. Clin. Invest.* **67:** 1712–1723.

35. Verma, M., and E. A. Davidson. 1994. Mucin genes: structure, expression and regulation. *Glycoconj. J.* **11:** 172–179.

36. Kim, Y. S., and J. R. Gum, Jr. 1995. Diversity of mucin genes, structure, function, and expression. *Gastroenterology.* **109:** 999–1001.

37. Gendler, S. J., and A. P. Spicer. 1995. Epithelial mucin genes. *Annu. Rev. Physiol.* **57:** 607–634.

38. Afdhal, N. H., N. Niu, D. Gantz, D. M. Small, and B. F. Smith. 1993. Bovine gallbladder mucin accelerates cholesterol monohydrate crystal growth in model bile. *Gastroenterology.* **104:** 1515–1523.

39. Wang, D. Q., F. Schmitz, A. S. Kopin, and M. C. Carey. 2004. Targeted disruption of the murine cholecystokinin-1 receptor promotes intestinal cholesterol absorption and susceptibility to cholesterol cholelithiasis. *J. Clin. Invest.* **114:** 521–528.

40. Toor, E. W., D. F. Evans, and E. L. Cussler. 1978. Cholesterol monohydrate growth in model bile solutions. *Proc. Natl. Acad. Sci. USA.* **75:** 6230–6234.